Supplementary Material
High-Affinity Binding and Direct Electron Transfer to Solid Metals by Purified Metal Reducing Protein OmcA Decaheme Cytochrome.

Yijia Xiong[1], Liang Shi[1], Baowei Chen[1], M. Uljana Mayer[1], Brian H Lower[2], Yuri Londer[2], Saumyaditya Bose[2], Michael F. Hochella[2], James K. Fredrickson[1,2], and Thomas C. Squier[1]

[1]Division of Biological Sciences and [2]Environmental Molecular Science Laboratory Biogeochemisty Grand Challenge Program; Pacific Northwest National Laboratory, Richland, WA 99352

RECEIVED DATE (automatically inserted by publisher); thomas.squier@pnl.gov

Institutional Affiliations of Biogeochemistry Grand Challenge Team:

Saumyaditya Bose and Michael F. Hochella: Department of Geosciences, Virginia Polytechnical Institute, Blacksburg, VA 24061.

Yuri Y. Londer: Biosciences Division, Argonne National Laboratory, 9700 South Cass Avenue, Argonne, IL 60439.

Brian H. Lower* and James K. Fredrickson+: Chemical* or Biological+ Sciences Divisions, Fundamental Sciences Directorate, Pacific Northwest National Laboratory, Richland, WA 99352.

OmcA and Experimental Buffer: Wild-type recombinant OmcA was expressed with V5 and His_6 tags at the C-terminus, and was purified using immobilized metal affinity columns (IMAC).[2a] No additional tags (e.g., tetracysteine tags) were employed in these measurements. OmcA (85 μg/mL or 1.0 μM) in 20 mM HEPES (pH 7.5), 0.15 M NaCl, and 8 mM CHAPS (CMC = 8-10 mM) was used in all experiments. In all cases, hematite was preincubated in 20 mM HEPES (pH 7.5), 0.15 M NaCl, and 8 mM CHAPS and the detergent concentration was kept constant. Similar OmcA binding to hematite was observed when the lipid binding site near the N-terminus of the protein was truncated (in the absence of added detergent), ensuring that binding to hematite was specifically associated with the functional properties of OmcA and its ability to transfer electrons directly to hematite.

Hematite Synthesis: Hematite nanoparticles were synthesized as previously described.[8] Briefly, this involved slowly dripping 60 mL of 1 M ferric nitrate solution into 750 ml of boiling ultrafiltered and doubly distilled MilliQ water. After the drip solution was consumed, the nanoparticle solution was removed from the heat and the synthesis suspension was cooled overnight. The nanoparticle solution was then dialyzed in high grade regenerated cellulose tubular membranes (Cellu Sep H1, 6000-8000 molecular weight cut-off) against doubly distilled MilliQ water until the conductivity of the dialysis water reached that of pure MilliQ. The suspensions were then poured into HDPE bottles for storage. Some of the suspension was freeze dried in a Labconco FreeZoen freeze dry system prior to characterization.

Hematite Characterization: Mineralogical characterization was carried out by powder X-ray diffraction **(XRD)** on a Philips X'Pert MPD system with a Cu anode operating at a wavelength of 1.5406Å ($CuK\alpha_1$) as the radiation source (see below). Specimens were prepared by grinding the samples in an agate mortar and pestle to fine powder and then placed on off axis quartz plates (18mm dia x 0.5 mm DP cavity). Diffraction patterns were recorded with a proportional counter detector over a 10-60° two theta scan range at a rate of 0.025°/sec. The X-ray diffraction powder pattern revealed the synthetic samples to be pure hematite with no detectable amounts of impurities.

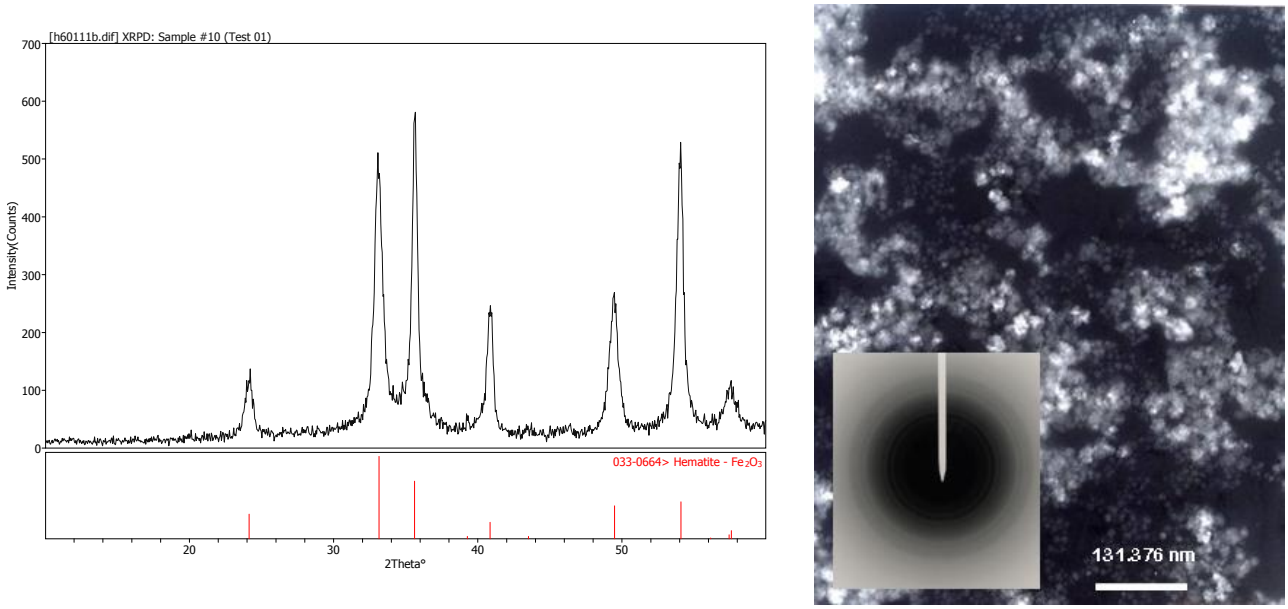

Powder X-ray diffraction pattern (left) and transmission electron micrograph (right) of hematite nanoparticles.

Particle morphology, size distribution, and electron diffraction patterns were obtained by transmission electron microscopy (TEM) (see above). Specimens were prepared by placing a drop of hematite suspension onto a 200 mesh formvar-coated copper grid (stabilized with evaporated carbon film) and allowed to evaporate. The products were observed in a Phillips EM 420T Scanning Transmission Electron Microscope operated in bright field mode at 100 KeV. Size distribution and morphology was estimated by observing approximately 90-100 particles from TEM negatives on a lightbox with a 10x magnifier with measuring scale. The TEM micrographs show aggregated pseudo-hexagonal platelets. Electron diffraction rings indicate hematite. The mean particle size and standard deviation as determined from a normal fit to the size distribution histogram was 11 ± 2 nm.

Specific surface area was determined by nitrogen gas adsorption by the Brunauer-Emmett-Teller (BET) method. The freeze-dried powder was degassed overnight at 100 °C followed by a 6-point BET isotherm in a Quantachrome Nova 1000 N_2 adsorption analyzer with N_2 as the adsorbate. The BET specific surface area was determined to be 95.95 (m^2/g).

Solubility of Hematite: The solubility of solid minerals is determined by the free energy of dissolution, which in general is very low for Fe(III) oxides (i.e., in the nanomolar range in the pH range between 4-10 in the absence of complexing agents). Indeed, minimum solubility is observed between pH 7 and pH 8; around pH 7.5 the solubility of hematite (the least soluble iron oxide) is approximately 5 pM independent of added salts[12]. Solubilities are enhanced for small particles, such that the calculated solubility of Fe(III) increases by about two order of magnitude upon decreasing the particle size to about 10 nm. However, even under these latter conditions the concentration of free Fe(III) in solution is substantially less than 1 nM. Thus, the concentration of free (unchelated) iron is less than 0.1% of the concentration of OmcA used in enzyme activity measurements (i.e., 1 uM), where electron transfer rates were 60 nmol/mg/min in the presence of hematite (Figure 1A). In comparison, prior activity measurements using soluble iron were made in the presence of 10 mM Fe(III)-NTA, and no measurable activity was detected in the absence of NTA[2a].

Reductase Activity of OmcA: The reductase activity of OmcA toward hematite was assayed using a variation of a previously described procedures.[1,13-15] Briefly, OmcA was chemically reduced by sodium dithionite. The reaction was carried out in anaerobic glass cells (STARNA, Atascadero, CA, USA), that contained purified OmcA (1 μM) in 1 mL of 20 mM HEPES (pH 7.5), 150 mM NaCl, 0.5% CHAPS, 10% glycerol and different concentrations of hematite, rotated in a Labquake tube rotator (Fisher, Pittsburg, PA, USA). The absorption spectrums, $OD_{540\text{-}560}$, of OmcA were recorded by an Agilent 8453 UV/Vis diode array spectrometer (Palo Alto, CA, USA) in an anaerobic chamber to measure the oxidation rate of OmcA by hematite. Controls included omission of hematite. All solutions were purged with 80% N_2/20% CO_2 (room temperature, 2 hr) before use, and all reactions were performed at room temperature in an anaerobic chamber with O_2 level of 1 ppm. After the initial rates (less than 10% of the hemes were oxidized) were calculated, they were fitted to the Michaelis-Menten equation to yield k_m and k_{cat} by using OriginPro7.5 software.

Covalent Attachment of Alexa-488 to OmcA: OmcA was fluorescently labeled using amine reactive Alexa Fluor® 488 carboxylic acid succinimidyl ester (cat #A20000, Invitrogen, Eugene, OR) at a molar stoichiometry of about 2:1 (dye to protein). Briefly, Alexa488 (40 μM)was incubated with OmcA [0.6 mg/ml in 10 mM Na_2PO_4 (pH 7.5), 150 mM NaCl, 0.5% CHAPS] for two hours at room temperature, and Alexa488-labeled OmcA was separated from free dye using size exclusion chromatography (i.e., a Sephedex G25 column) into 20 mM HEPES (pH 7.5), 150 mM NaCl and 0.5% CHAPS. The concentration of Alexa488 bound to OmcA was determined by its absorbance at 494 nm (ε_{494nm} = 73000 M^{-1} cm^{-1}).

Purification of SO0717: The predicted mature fragment of SO0717 was cloned as a C-terminal fusion to a hybrid 6 × His-Maltose binding protein affinity tag followed by a cleavage site for TEV protease.[16] The plasmid was transformed into *E. coli* strain BL21(DE3) harboring auxiliary plasmid pEC86 that contains genes for cytochrome *c* maturation.[17] *E. coli* cultures were grown aerobically to mid-exponential phase at 30°C and 250 rpm and induced with 20 μM IPTG. The incubation continued overnight at 30 °C and 200 rpm. Next morning the cells were harvested and resuspended in 100 mM Tris-HCl (pH 8.0), 20% sucrose, and 0.5 mM EDTA containing 0.5 mg/ml lysozyme and protease inhibitor cocktail for bacterial cells (Sigma). 30 ml of the buffer was used to resuspend a pellet from 1 L of culture. Resuspended cell were incubated at room temperature for 15 min. Then an equal volume of ice-cold 1 M NaCl solution was added and the cells were incubated on ice with gentle shaking for 15 min and centrifuged at 12,000 × *g* for 20 min at 4°C. The supernatant constituted the periplasmic fraction. Then imidazole and $MgCl_2$ were added to final concentrations of 5 mM and 2 mM, respectively, and the prep was purified on a 20 mL Ni Sepharose 6 Fast Flow (GE Healthcare) column equilibrated with buffer A [20 mM Tris-HCl (pH 8.0), 0.5 M NaCl, and 5 mM imidazole] according to the manufacturer's instructions. Then TEV protease was added in 1:20 (w/w) ratio and the sample was dialyzed overnight against buffer A. The dialyzed sample was loaded onto the same re-equilibrated Ni Sepharose 6 Fast Flow column and the flow-through was collected and dialyzed against 20 mM HEPES (pH 7.5) and 150 mM NaCl. The purified protein was frozen at – 80 °C prior to use.

ADDITIONAL REFERENCES:

Complete References for those Abbreviated in the Manuscript:

2a. Shi, L.; Chen, B.; Wang, Z.; Elias, D. A.; Mayer, M. U.; Gorby, Y. A.; Ni, S.; Lower, B. H.; Kennedy, D. W.; Wunschel, D. S.; Mottaz, H. M.; Marshall, M. J.; Hill, E. A.; Beliaev, A. S.; Zachara, J. M.; Fredrickson, J. K.; Squier, T. C., Isolation of high-affinity functional protein complex between OmcA and MtrC: Two outer membrane decaheme c-type cytochromes of *Shewanella oneidensis* MR-1. *J Bacteriology* **2006,** 188, 4705-4714.

2b. Gorby, Y. A.; Yanina, S.; McLean, J. S.; Rosso, K. M.; Moyles, D.; Dohnalkova, A.; Beveridge, T. J.; Chang, I. S.; Kim, B. H.; Kim, K. S.; Culley, D. E.; Reed, S. B.; Romine, M. F.; Saffarini, D. A.; Hill, E. A.; Shi, L.; Elias, D. A.; Kennedy, D. W.; Pinchuk, G.; Watanabe, K.; Ishii, S.; Logan, B.; Nealson, K. H.; Fredrickson, J. K., Electrically conductive bacterial nanowires produced by *Shewanella oneidensis* strain MR-1 and other microorganisms. *Proc Natl Acad Sci U S A* **2006,** 103, (30), 11358-11363.

2c. Marshall, M. J.; Beliaev, A. S.; Dohnalkova, A. C.; Kennedy, D. W.; Shi, L.; Wang, Z.; Boyanov, M. I.; Lai, B.; Kemner, K. M.; McLean, J. S.; Reed, S. B.; Culley, D. E.; Bailey, V. L.; Simonson, C. J.; Saffarini, D. A.; Romine, M. F.; Zachara, J. M.; Fredrickson, J. K., c-Type Cytochrome-Dependent Formation of U(IV) Nanoparticles by *Shewanella oneidensis*. *PLoS Biol* **2006,** 4, 1324-1333.

Additional References Not Already Cited:

12. Cornell, R.; Schwertmann, U., *The Iron Oxides: Structure, Properties, Reactions, Occurances and Uses.* WILEY-VCH Verlag GmbH & Co. KGaA, Weinheim.: 2003; p pp. 201-220.

13. Field, S. J.; Dobbin, P. S.; Cheesman, M. R.; Watmough, N. J.; Thomson, A. J.; Richardson, D. J., Purification and magneto-optical spectroscopic characterization of cytoplasmic membrane and outer membrane multiheme c-type cytochromes from *Shewanella frigidimarina* NCIMB400. *J Biol Chem* **2000,** 275, 8515-8522.

14. Magnuson, T. S.; Hodges-Myerson, A. L.; Lovley, D. R., Characterization of a membrane-bound NADH-dependent Fe(3+) reductase from the dissimilatory Fe(3+)-reducing bacterium Geobacter sulfurreducens. *FEMS Microbiol Lett* **2000,** 185, 205-211.

15. Pitts, K. E.; Dobbin, P. S.; Reyes-Ramirez, F.; Thomson, A. J.; Richardson, D. J.; Seward, H. E., Characterization of the *Shewanella oneidensis* MR-1 decaheme cytochrome MtrA: expression in Escherichia coli confers the ability to reduce soluble Fe(III) chelates. *J Biol Chem* **2003,** 278, 27758-27765.

16. Donnelly, M. I.; Zhou, M.; Millard, C.S.; Clancy, S.; Stols, L., Eschenfeldt WH, Collart FR, Joachimiak A. An expression vector tailored for large-scale, high-throughput purification of recombinant proteins. *Protein Expr Purif.* **2006,** 47, 446-454.

17. Arslan, E.; Schulz, H.; Zufferey, R.; Kunzler, P.; Thöny-Meyer, L., Overproduction of the *Bradyrhizobium japonicum c*-type cytochrome subunits of the cbb_3 oxidase in *Escherichia coli*. Biochem Biophys Res Commun **1998,** 251, 744–747.

18. Stipp, S. L.; Hochella, M. F., Jr., Structure and bonding environments at the calcite surface as observed with X-ray photoelectron spectroscopy (XPS) and low energy electron diffraction (LEED). *Geochimica et Cosmochimica Acta* **1991,** 55, 1723-1736.

19. Lower, S.K., Hochella, M.F., Jr. and Beveridge, T.J. Bacterial recognition of mineral surfaces: nanoscale interactions between *Shewanella* and alpha-FeOOH. *Science* **2001**, 292, 1360-1363.

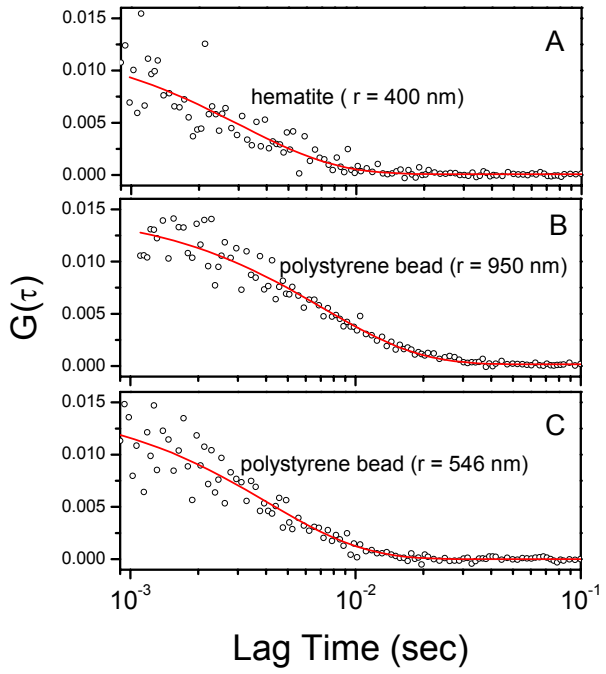

Figure S1. Average spherical radius determined from fits (red lines) to dynamic light scattering (DLS) data (circles) for (A) hematite in 20 mM HEPES (pH 7.5), 150 mM NaCl, and 0.5% w/v CHAPS in comparison to data collected for polystyrene bead standards whose radii are known to be 950 nm (Fluosphere cat #F8887, Molecular Probes, Eugene OR) (B) or 545 nm (Polystyrene bead cat #16905, Polysciences Inc, Warrington PA) (C). The normalized experimental curve was fit to the following: $G(t) = A \times \exp[-2D_t q2t]$, where A is an instrumental coefficient, D_t is the translational diffusion coefficient, and q is the scattering vector $[4\pi n \sin(\theta/2)/\lambda]$, where n is the refract index, θ is the scattering angle and λ is the wavelength of the scattering light (λ_{ex} = 633 nm). The apparent radius (r) for a spherical particle was calculated from the Stokes-Einstein equation $r = kT / 6\pi\eta D_t$, where r is the hydrodynamic radius of the molecule, k is the Boltzmann constant (1.38×10^{-23} *J/K)*, T is the absolute temperature (293 ºK), and η is the viscosity of water (0.001 kg/m/s, or 0.01 poise). From the data the average radius of hematite was approximately 400 nm (A), while that of the polystyrene beads were respectively determined to be 950 nm (B) and 546 nm (C).

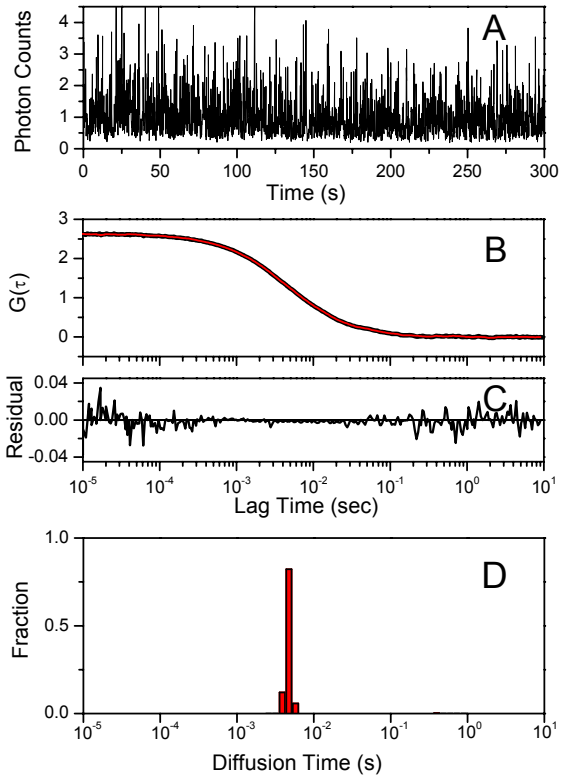

Figure S2. Fluorescence intensity traces (A) and derived experimental correlation curve (black) and fit (red) (B), residuals of the fitting (C), and the distribution of diffusion times (τ_D) (D) calculated using an aqueous suspension of standard beads with a known radius of 50.5 nm that was labeled with a red fluorophore (FluoSpheres F8887, 580/605, Molecular Probes Inc. Eugene OR). The translational diffusion coefficient (D_t) calculated from:

$$D_t = \frac{\omega^2}{4 \times \tau_D}$$, where for $\tau_D = 4.4 \times 10^{-3}$ s one can calculate that $D_t = 4.1 \times 10^{-8}$ cm^2 / s.

From the Stokes-Einstein equation the radius (r) of a spherical particle can be calculated according to:

$$r = \frac{kT}{6\pi\eta D_t} = \frac{(1.38\times10^{-16}\,\text{dyne cm deg}^{-1})(293°\text{K})}{6\pi\,(0.01\,\text{dyne sec cm}^{-2})(4.1\times10^{-8}\,\text{cm}^2\,\text{sec}^{-1})} = 52\ \text{nm}$$

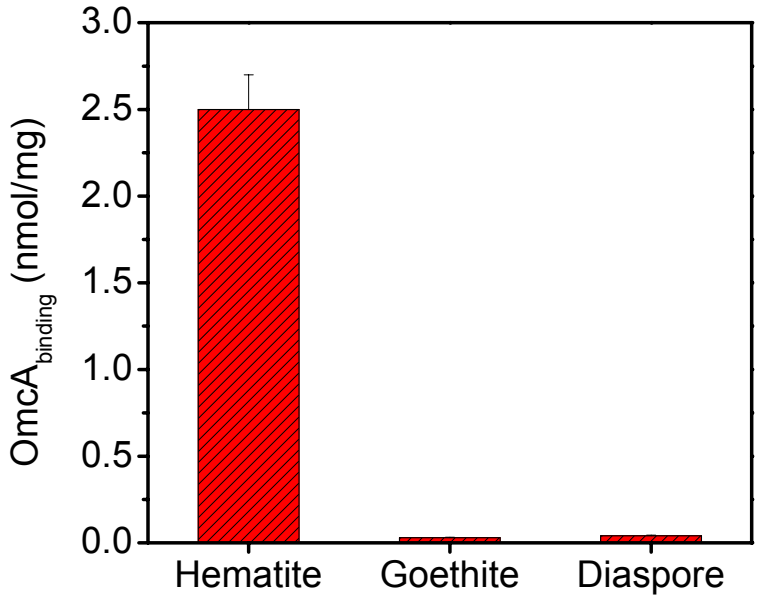

Figure S3. Loss of OmcA through co-sedimentation with hematite (α-Fe_2O_3), goethite (α-FeOOH) and diaspore (α-AlOOH) particles following centrifugation (16,000 x g for 10 min) following addition of 0.16 mg/mL hematite or 1.6 mg/mL goethite or diaspore. Buffer is 20 mM HEPES (pH 7.5), 150 mM NaCl, and 0.5% w/v CHAPS. Natural samples of goethite and diaspore were obtained from the Department of Geosciences Museum at Virginia Tech. Each sample was crushed and wet sieved through a 45 µm sieve. Those particles passing through the filter were collected and cleaned of adventitious carbon[18], and confirmed to be solely composed of either goethite or diaspore by X-ray diffraction analysis.

Our results, demonstrating a functional and high-affinity interaction between OmcA and hematite suggests a direct role for this metal reductase in mediating electron transfer to hematite. The lack of binding of purified OmcA to goethite is in contrast to prior measurements using living *Shewanella* that demonstrated a high affinity interaction with goethite under anaerobic conditions when metal reductases are highly expressed in the outer membranes of *Shewanella*[19]. However, no prior measurements considered the ability of a purified metal reductase to bind and transfer electrons to solid minerals, and the nature of the bacterial-mineral interaction remains unclear and could involve nonspecific interactions involving, for example, polysaccharides. The inability of OmcA to bind to goethite is consistent with our prior suggestions that functional binding interactions between multiple metal reductases (e.g., OmcA and MtrC) function to enhance binding affinities between *Shewanella* and different minerals.[2a] Future measurements will endeavor to document the binding interactions between different metal reductases and the range of minerals in soils that are used as electron transfer acceptors in the colonization of soils by *Shewanella* and other metal reducing bacteria.

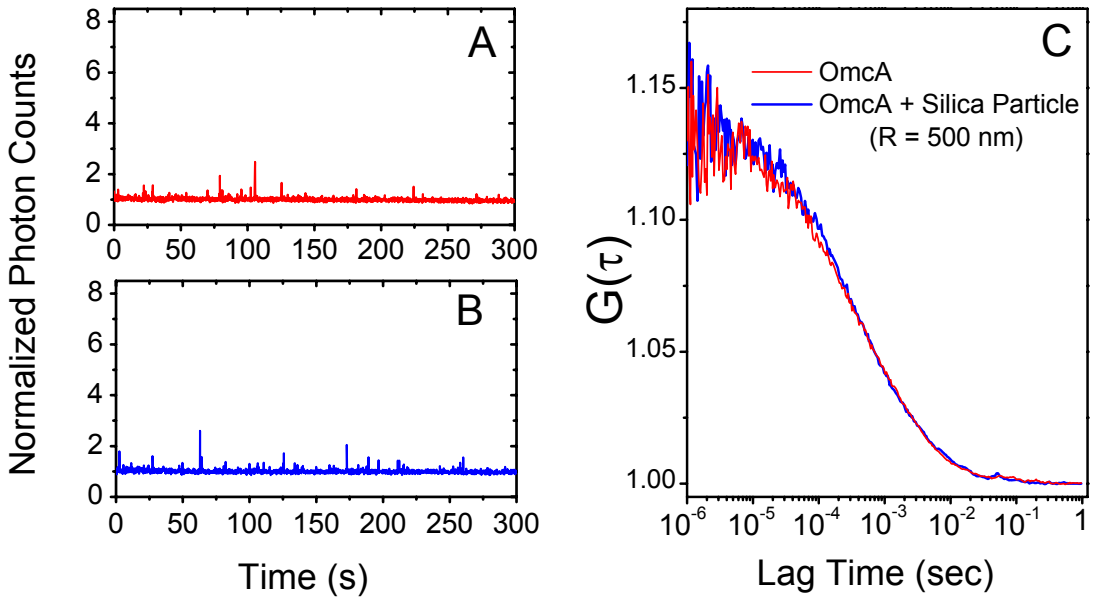

Figure S4. Fluorescence intensity traces for 100 nM Alexa488-labeled OmcA in the absence (A) or presence (B) of silica microspheres (100 μM) (R = 500 nm; Polysciences Inc., Cat # 24323) and their fluorescence correlation spectroscopy curves(C), respectively. Buffer is 20 mM HEPES (pH 7.5), 150 mM NaCl, and 0.5% w/v CHAPS.

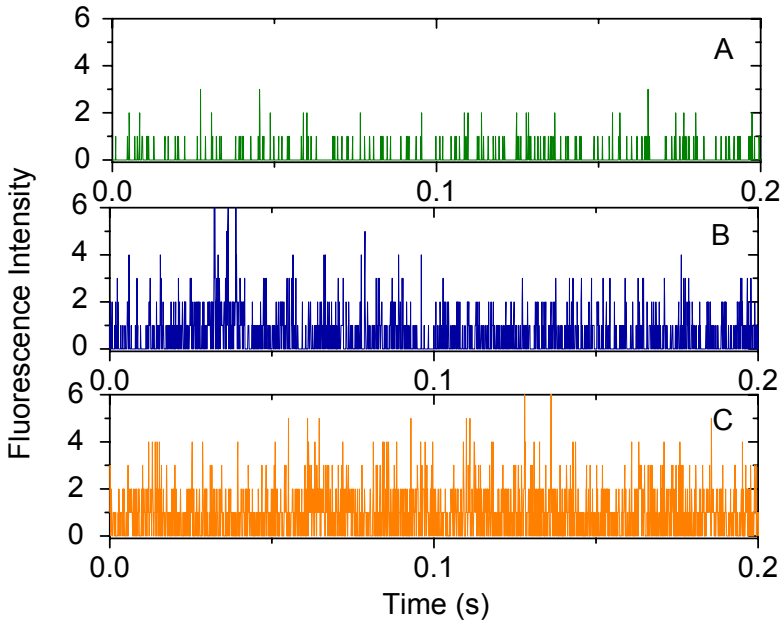

Figure S5. Fluorescence intensity trace of 10 nM (A), 50 nM (B) and 100 nM (C) Alexa488-labeled OmcA in 20 mM HEPES (pH 7.5), 150 mM NaCl, and 0.5% w/v CHAPS. In all cases, the sample time was 100 μs.

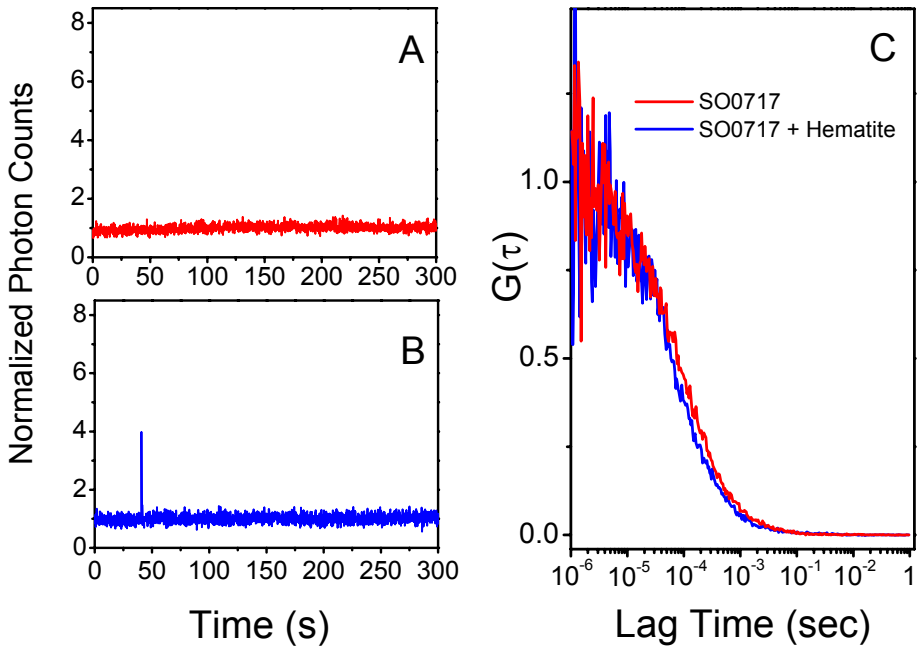

Figure S6. Fluorescence intensity traces for 100 nM Alexa488-labeled SO0717 in the absence (A) or presence (B) of hematite (16 μg/ml) and their fluorescence correlation spectroscopy curves (C), respectively. Buffer is 20 mM HEPES (pH 7.5) and 150 mM NaCl. SO0717 is a cytochromes containing protein isolated from *Shewanella oneidensis*.